MULTI-CHANNEL SUBTRACTIVE SPECTROGRAPH AND FILAMENT OBSERVATIONS

P. MEIN
Observatoire de Paris-Meudon, 92190 *Meudon, France*

(Received 1 March, 1977)

Abstract. A Multi-Channel Subtractive Double Pass spectrograph (MSDP) has been achieved at the Meudon solar tower. Line profiles are obtained simultaneously in a two dimensional field. Space and time resolutions are very suitable for observation of fast chromospheric phenomena.

Maps have been computed for Doppler shifts and Hα-intensities (core and wings) in a plage including a temporary activated filament. The radial velocity is zero in the core of the filament, but it increases toward the edges with opposite signs on the both sides. Velocity loops inclined at small angles on the axis of the filament are suggested.

1. Introduction

Many attempts have been made to observe line profiles in two-dimensional fields; fast scanning of the Sun with the slit of a spectrograph, wavelength scannings with a narrow-band filter. In any case, the observations are not simultaneous. Multi-slit or slicer systems have also been used. They give a high spectral resolution, but a low space definition. In the case of strong or middle-strong lines, it is possible to get a high space definition, with a spectral resolution which is good enough to allow Doppler-shift measurements. This is obtained with the 'Multi-Channel Subtractive Double Pass' spectrograph (MSDP) described in this paper.

A few years ago, optical systems using the reversal of the dispersion between the first and the second pass on the grating of a spectrograph had been developed in Capri (Stenflo, 1968, 1973) and Meudon (Mein and Blondel, 1972). But such instruments could only give one or two pictures of the same field simultaneously. In particular, it was impossible to restore the whole profile of a line over the whole field. The new Meudon instrument records 7 wavelengths in the whole field at the same time. The space resolution is limited only by seeing effects. The spectral resolution is 0.36 Å presently, and will be better in the future.

2. Description of the MSDP Spectrograph

The optical system is similar to the two-channel version (Mein and Blondel, 1972). The field is unchanged (rectangular window $\sim 4' \times 40''$). But in the focal plane of the first spectrum N equidistant slits ($N = 7$ presently) are followed by a set of N prisms which shift the beams without any modification of the focus. After the second pass on the grating, N 'channels' or images of the entrance window are collected on the 70 mm-film. Figure 1 shows an example of such multi-channel

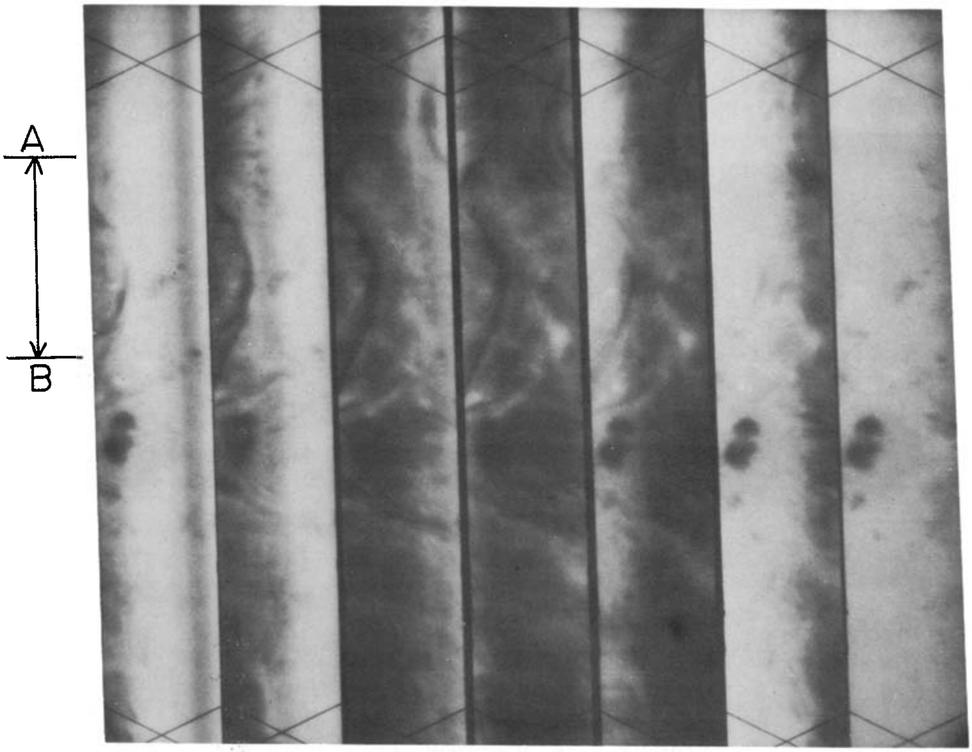

Fig. 1. An active region filament observed with the MSDP of the Meudon solar tower in the Hα-line, August 7, 1975. The total field is about $240'' \times 37''$.

picture, which will be analysed below. Let us call x, y the space coordinates on the Sun (x parallel to the dispersion direction) and λ the wavelength. We have plotted on Figure 2 the wavelength of the photons as a function of x for the N channels (λ does not depend on y). If n is the channel number, $1/\alpha$ the dispersion of the spectrograph (identical in the first and second pass), ε the wavelength distance between two slits, w the width of each slit, and λ_0 a constant depending on the grating angle, λ is given by

$$\lambda = \lambda_0 - n\varepsilon + \alpha x \pm w/2. \tag{1}$$

In the whole field ($0 < x < X, 0 < y < Y$), the spectrum is obtained with the wavelength resolution ε in the minimum range R defined by

$$\lambda_0 - N\varepsilon + \alpha X < \lambda < \lambda_0 - \varepsilon. \tag{2}$$

In the Meudon spectrograph $X = 8$ mm, $1/\alpha = 8.3$ mm/Å, $\varepsilon = 0.36$ Å, $w = 0.18$ Å and $R = 1.2$ Å for the Hα line.

3. Capabilities

Let us compare the MSDP instrument to a standard spectrograph and to a narrow-band filter. On Figure 2 a spectrograph would be represented by only one

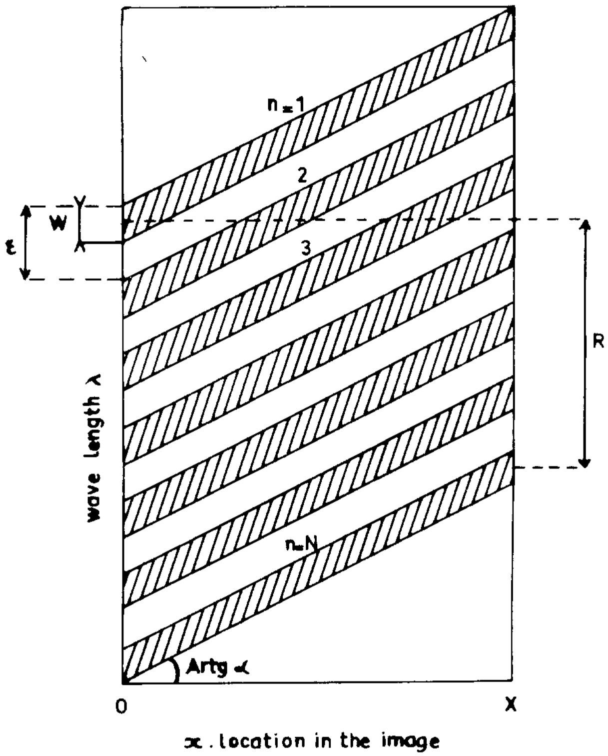

Fig. 2. Wavelength versus the x-coordinate on the Sun for the N channels of the MSDP. Hatched areas show the photons which are recorded simultaneously.

straight line parallel to the λ-axis, and a filter would be represented by only one straight line parallel to the x-axis. The MSDP comes out to be *the most efficient technique* with respect to the *number of useful photons recorded simultaneously. Two-dimensional fast phenomena* can be observed with a time resolution limited only by the exposure time (1.7 s in Meudon on Plus X 2402 film, in spite of atmospheric absorption).

Moreover, the space resolution is not smoothed by any slit-width as in a classical spectrograph. Generally, it is *limited only by the seeing quality* which is very interesting for the *observations of fine structures.*

It must be noted also that the simultaneous observation of all the points in the line *avoids difficulties due to distortion by seeing effects in the profile restoration,* and that the local wavelength pass band is rectangular, which leads to a well defined spectral analysis.

4. Processing of data

The observations have been processed in the following way:

(a) The film is scanned with a fast microdensitometer (PDS) using a square aperture ($0.4'' \times 0.4''$). About 0.5×10^6 measurements are recorded for one picture.

(b) In order to correct slight translations, rotations and size differences between the channels, the accurate location of the crosses of hair-lines recorded on each one are computed (accuracy better than 0.1″). The final space resolution is 0.8″ in both directions.

(c) Photometric corrections are applied in order to compensate small transmission departures between the channels (function of n) and between the different y-location in each channel (a small angle between slits and prisms leads to linear intensity fluctuations). At the same time, telluric lines of water vapour which could disturb Doppler-shift determinations are eliminated (functions of x). For this purpose, a two-gaussian function $Q(\lambda)$ is fitted to the Hα mean profile

$$P(x, n) \equiv P(\lambda - \lambda_0 + n\varepsilon/\alpha, n) \tag{3}$$

deduced from an average of many different pictures (or one picture out of focus). The difference Q-P leads to the correction function, after averaging over x the terms which depend on y, and averaging over y the terms which depend on x.

(d) Around the inflexion point, an estimation of the contrast factor of the film can be deduced from fitting the slope of the observed mean profile to the standard quiet profile. Velocity calculations are independent on the photometric calibration.

(e) The line profile is restored in each point of the Sun by interpolations.

(f) Velocity and intensity maps are computed in a way very similar to 'lambdameter' measurements. For a given $\Delta\lambda$-value, the couple of points of equal intensity separated by the wavelength distance $2\Delta\lambda$ is determined by an iterative process. The noise is the lowest one when the $2\Delta\lambda$-value is approximately the distance of the inflexion points of the line profile.

5. Velocity Field in an Active Region Filament

(a) Results

An active region was observed at the Meudon solar tower on August 7, 1975 at 16 h 17 m UT (30°W, 7°N). A filament lies in the Hα facula (Figure 1). Maps have been plotted on Figure 3 for the part of the field noted A-B in Figure 1: intensity fluctuations I_1 and I_2 correspond to $\Delta\lambda = 0$ and $\Delta\lambda = 0.45$ Å, Doppler shifts V correspond to $\Delta\lambda = 0.45$ Å. Continuous lines refer to bright regions or downward velocities, dashed lines refer to dark regions or upward velocities.

It comes out that the radial velocity is zero in the axis of the filament, and increases very rapidly in the edges. The velocity remains downward on one side and upward on the other side, over a wide range along the filament. Local maxima are 5.5 km s^{-1} (point M_1), $-7(N_1)$, $4(M_2)$, $-6.5(N_2)$. Outside the filament, the radial velocity is generally low. Figure 3d shows a map of the function

$$G = \left(\left(\frac{\partial V}{\partial x}\right)^2 + \left(\frac{\partial V}{\partial y}\right)^2\right)^{1/2},$$

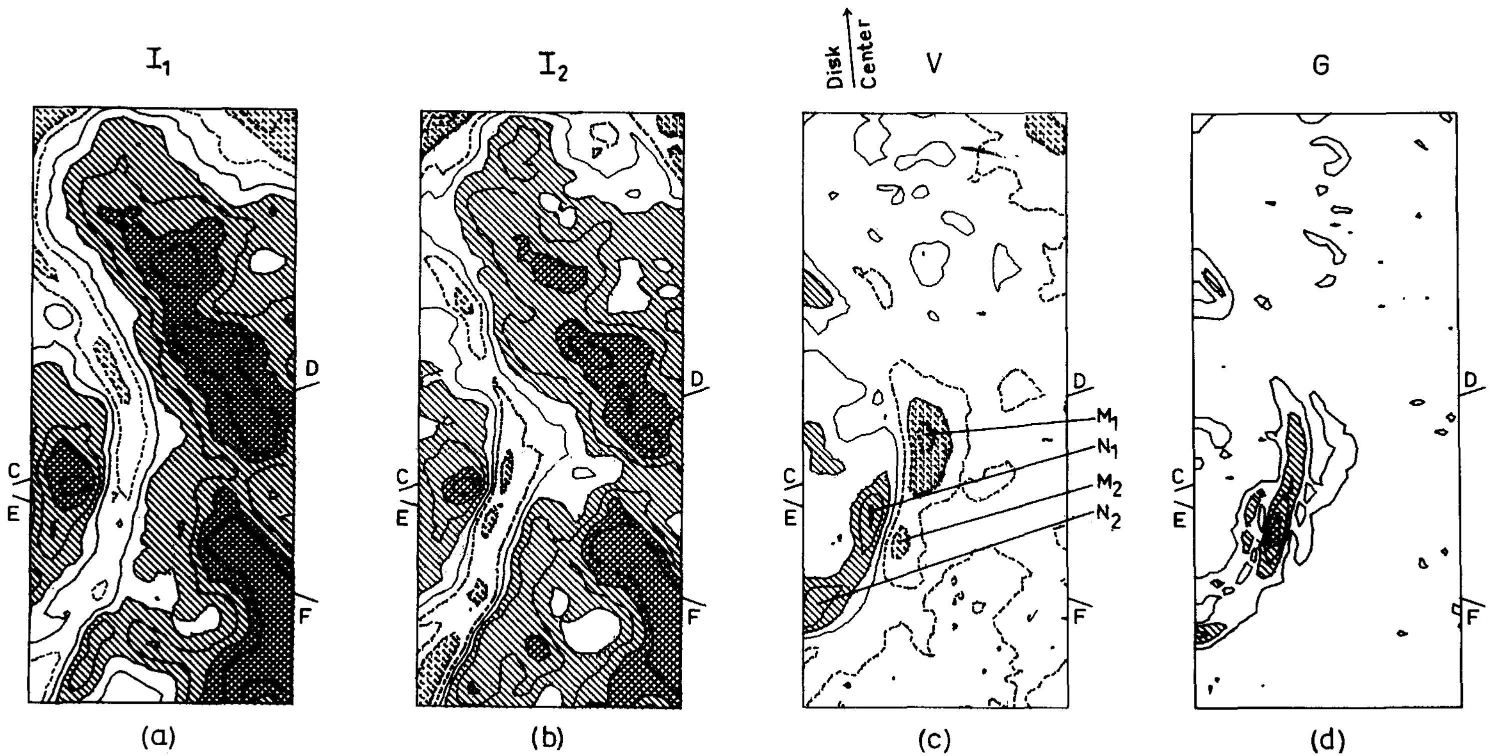

Fig. 3. Maps of Hα-intensity fluctuations ($I_1, \Delta\lambda = 0$; $I_2, \Delta\lambda = 0.45$ Å) and Doppler shifts ($V, \Delta\lambda = 0.45$ Å) for the field defined by AB in Figure 1. Continuous lines refer to bright regions, or downward velocities. The G-function is defined in the text. The levels correspond to $\Delta \log I_1 = \pm 0.03, 0.09, 0.15, 0.21, 0.27$; $\Delta \log I_2 = \pm 0.02, 0.06, 0.10, 0.14, 0.18$, $V = \pm 1, 3, 5, 7$ km s^{-1}; $G = 1, 2, 3, 4, 5$ km s^{-1} arc sec^{-1}

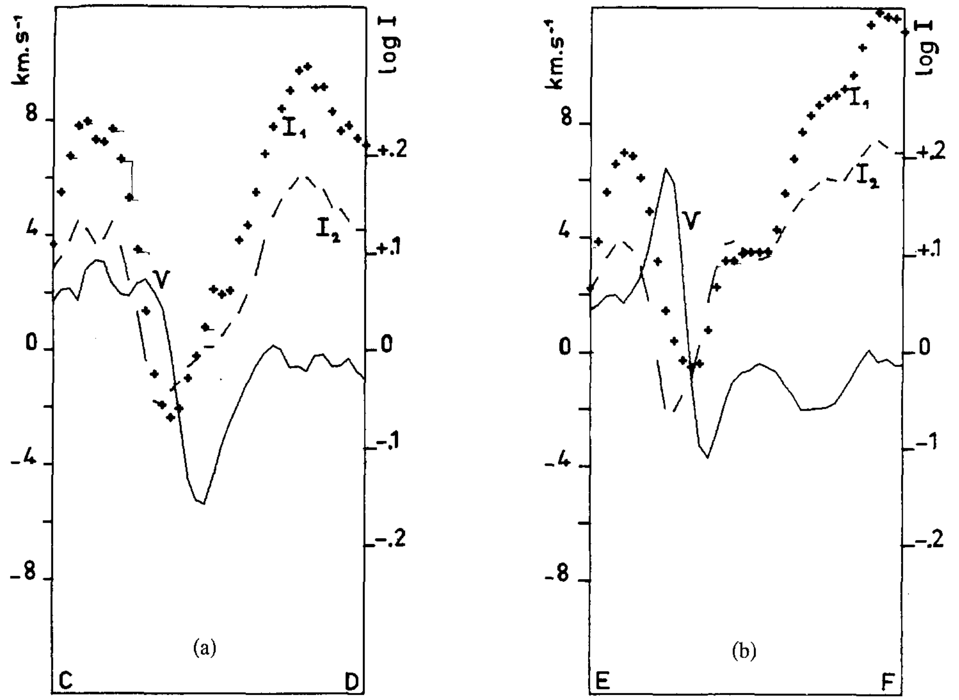

Fig. 4. Velocities V (continuous line) and intensity fluctuations I_1 (crosses) and I_2 (dashed line) along CD and EF (see Figure 3). Note that high velocities take place inside the filament.

which describes the horizontal variation of the radial velocity. This function is maximum in the core of the filament. In order to localize the high velocities with respect to the absorbing filament, the functions I_1, I_2 and V have been plotted on Figures 4a and 4b along two lines approximately perpendicular to the axis (CD and EF respectively). It is obvious that the highest velocities occur inside the dark material.

(b) Discussion

This active region filament cannot be compared to the quiescent prominence analysed by Maltby (1976). It was observed also by filtergram technique in Meudon from August 3. On August 7, it was stable early in the morning, but very much activated during the day, and associated with many flares. It was not seen anymore on August 8. From previous works by Smith (1968), it could be expected that material flows take place along the filament (Tandberg-Hanssen, 1974). At first sight, it would seem that our observations disagree with this description, since upward and downward velocities happen near the same point of the axis. Strictly speaking, we do not know if the material is flowing along or across the filament, because we measure the radial component of the velocity only. Nevertheless, we can notice that the fine structure of the filament (Figure 1) suggests elongated features slightly inclined with respect to the axis of the filament, according to a direction which could be parallel to M_1N_1 (or M_2N_2). Moreover, if we assume that velocity loops do exist between M_1 and N_1 (and M_2-N_2) with inclined directions at the feet in the chromosphere, the perspective effect can account qualitatively for a downward velocity greater than the upward velocity. The time which would be necessary to go from M_1 to N_1 along a circular loop with a 10 km s^{-1} velocity is around 20 mn. It can be compared to the lifetime of a temporaty activation.

For a given size of the loops and a given material velocity along them, the G-function increases when the angle between the axis of the filament and the plane of the loops decreases. Since the maximum of G is rather sharp and occurs in the core of the filament, it may be suggested that the loops are not plane, but S-shaped, with the inflexion point on the axis of the filament.

6. Conclusion

The Multi-Channel Subtractive Double Pass technique is very suitable for observation of time-dependent chromospheric structures. Maps of velocities and line intensities are obtained simultaneously at the Meudon solar tower, with a few second intervals between two successive frames. The space resolution is not affected by any slit-width in the instrument.

Preliminary results have been obtained for a temporary activated filament. The radial velocity is zero in the axis of the filament, but reaches high opposite values in the edges. Velocity loops crossing the filament inside the absorbing material can be suggested.

Acknowledgements

We want to express our thanks to M.-J. Martres and I. Soru-Escaut for observations with the MSDP, analysis of filtergrams and helpful discussions. We are indebted to A. Miguel, C. Coutard and R. Hellier for technical assistance in instrumental problems.

We thank also the technical staff of the Meudon Observatory, the Centre de Dépouillement de Clichés Astronomiques in Nice and the Centre de Calcul de l'INAG in Meudon.

References

Maltby, P.: 1976, *Solar Phys.* **46,** 149.
Mein, P. and Blondel, M.: 1972, *Solar Phys.* **27,** 489.
Smith, S. F.: 1968, in K. O. Kiepenheuer (ed.), 'Structure and Development of Solar Active Regions', *IAU Symp.* **35,** p. 267.
Stenflo, J. O.: 1968, *Solar Phys.* **3,** 482.
Stenflo, J. O.: 1973, *Appl. Opt.* **12,** 805.
Tandberg-Hanssen, E.: 1974, *Solar Prominences*, D. Reidel Publ. Co., Dordrecht-Holland, p. 27.